

OBSERVATIONAL MATTER POWER SPECTRUM AND THE HEIGHT OF THE SECOND ACOUSTIC PEAK

F. ATRIO-BARANDELA

Física Teórica. Facultad de Ciencias
 Universidad de Salamanca, 37008 Spain
 e-mail: atrio@orion.usal.es

J. EINASTO

Tartu Observatory, EE-61602 Estonia
 e-mail: einasto@aai.ee

V. MÜLLER, J. P. MÜCKET

Astrophysikalisches Institut Potsdam
 An der Sternwarte 16, D-14482 Potsdam, Germany
 e-mail: (vmueller, jpmuecket)@aip.de

A. A. STAROBINSKY

Research Center for the Early Universe, University of Tokyo, Tokyo 113-0033, Japan and
 Landau Institute for Theoretical Physics, Moscow 117334, Russia
 e-mail: alstar@landau.ac.ru

Draft version October 24, 2018

ABSTRACT

We show that the amplitude of the second acoustic peak in the newly released BOOMERANG-98 and MAXIMA-I data is compatible with the standard primordial nucleosynthesis and with the locally broken-scale-invariant matter power spectrum suggested by recent measurements of the power spectrum in the range $20 - 200 h^{-1}$ Mpc. If the slope of matter density perturbations on large scales is $n \approx 1$, the Hubble constant is $0.5 < h < 0.75$, and r.m.s. mass fluctuations at $8 h^{-1}$ Mpc are $0.65 \leq \sigma_8 \leq 0.75$, then for a Universe approximately 14 Gyr old our best fit within the nucleosynthesis bound $\Omega_B h^2 = 0.019 \pm 0.0024$ requires $0.3 \leq \Omega_m \leq 0.5$. Cluster abundances further constraint the matter density to be $\Omega_m \approx 0.3$. The CMB data alone are not able to determine the detailed form of the matter power spectrum in the range $0.03 < k < 0.06 h \text{ Mpc}^{-1}$ where deviations from the scale-invariant spectrum are expected to be most significant, but they do not contradict the existence of the previously claimed peak at $k \sim 0.05 h \text{ Mpc}^{-1}$, and a depression at $k \sim 0.035 h \text{ Mpc}^{-1}$.

Subject headings: cosmic microwave background – cosmology: theory – cosmology: observations

1. INTRODUCTION

The recently released data from BOOMERANG-98 (de Bernardis et al. 2000, hereafter B00) and MAXIMA-I (Hanany et al. 2000) have determined the amplitude and position of the first and second acoustic (Doppler) peaks of the Cosmic Microwave Background (CMB) radiation angular spectrum. The first analysis (Balbi et al. 2000; Lange et al. 2001; Jaffe et al. 2000) strongly constrained the parameter space of cosmological models. The data clearly displayed a large first acoustic peak with the maximum at $l = l_{max} = 212 \pm 7$ (Bond et al. 2000) that supported the idea of an approximately spatially flat Universe with a cosmological constant (vacuum energy) and non-baryonic cold dark matter (CDM). However, rather unexpectedly, the second acoustic peak at $l \sim 500 - 550$ appears to have a low amplitude (especially in the B00 data). Another unexpected feature was a shift of the first peak to smaller l than the standard theoretical prediction $l_{max} \simeq 220$ for the flat Λ CDM model. Even more recently, Netterfield et al. (2001, hereafter B01), Lee et al. (2001, hereafter M01) have estimated the radiation power spectrum up to $l \sim 1100$ by extending the analysis of BOOMERANG-98 and MAXIMA-I data to smaller angular scales. Halverson et al. (2001, hereafter D01) presented the angular power spectrum from the first season of DASI observations with data out to $l \sim 800$.

A straightforward fit of the earlier data to Λ CDM mod-

els with a scale-invariant initial spectrum of adiabatic perturbations lead to:

a) a high best fit value of the baryon density $\Omega_B h^2 \approx 0.03$ (see, e.g., Tegmark & Zaldarriaga 2000b; Jaffe et al. 2000) that significantly exceeds the prediction of the standard Big-Bang nucleosynthesis (BBN), updated for the recent data on the primordial deuterium abundance: $\Omega_B h^2 \approx 0.019 \pm 0.0024$ (Tytler et al. 2000);

b) a best fit for the density $\Omega_{tot} \approx 1.1$ that corresponds to a closed Universe (Lange et al. 2001, Jaffe et al. 2000) (though the flat Universe is inside the 2σ error bars).

The former result is mainly the consequence of the low amplitude of the second acoustic peak, while the latter is mostly due to the shift of the first peak to the left. These conclusions persist if additional information on the Large Scale Structure (LSS) of the Universe, as the density fluctuation parameter σ_8 , and the shape of the power spectrum of matter are taken into account. In particular, the most exhaustive of these efforts made by Tegmark, Zaldarriaga & Hamilton (2000), who performed an 11-parameter fit to the current CMB and LSS data, has led to essentially the same result about the high baryon density. To avoid contradiction with the standard BBN, a number of drastic changes in the standard FRW cosmology were proposed, as leptonic asymmetry (Lesgourgues & Peloso 2000), delayed recombination (Peebles, Seager & Hu 2000), loss of coherence of primordial perturbations remained from inflation (White, Scott & Pierpaoli 2000), admixture of topological

defects (Bouchet et al. 2000) or even the absence of dark non-baryonic matter (McGaugh 2000). Moreover, even the fundamental laws of physics itself, as the constancy of the fine structure constant, have been abandoned for the sake of explaining these features (Avelino et al. 2000, Battye et al. 2001).

A preliminar study of the newest D01 data shows no contradiction with the BBN bound; B01 agrees with the earlier analysis of Lange et al (2001) except that the baryon abundance is reduced to $\Omega_b h^2 = 0.027 \pm 0.005$. This limit gets even closer to the BBN estimates if all points are considered in the analysis. But at high multipoles, the data is not fully consistent. M01 data show a third peak higher than the second, while in B01 and D01 both acoustic peaks are of similar height.

All studies quoted above, even those including information on LSS, considered matter power spectra only with scale-invariant initial conditions. But Einasto et al. (1999c) have shown that the matter power spectrum as measured from galaxy and cluster catalogs is inconsistent with this assumption. A number of different non-scale-invariant initial conditions has been recently used to analyze the CMB data. First, Kanazawa et al. (2000) considered a double inflationary model in supergravity having a step in the spectrum located around $k = 0.03 h \text{ Mpc}^{-1}$, for which both the matter power at smaller scales and the amplitude of the second Doppler peak are reduced. A similar matter spectrum was studied in Barriga et al. (2000) which resulted from another kind of inflationary model with a fast phase transition during inflation. In contrast, Griffiths, Silk & Zaroubi (2000) and, most recently, Hannestad, Hansen & Villante (2000) advocated the existence of a bump in the matter spectrum on significantly larger scales ($k \approx 0.004 h \text{ Mpc}^{-1}$) based on purely phenomenological grounds. Einasto (2000) analyzed the CMB spectrum resulting from a matter power spectrum with a bump at $k = 0.05 h \text{ Mpc}^{-1}$ as suggested by Chung et al. (2000).

In most of these papers, the location of non-scale-invariant features in the spectrum, or even the functional form of these features were introduced *ad hoc*, with the only aim to explain the BOOMERANG-MAXIMA early data. In contrast, we adopt a completely different approach: without attaching ourselves to any particular theoretical model, we are trying to use previously existing observational data as much as possible. To obtain the initial (post-inflation) matter spectrum, first, we use the empirical present matter power spectrum of Einasto et al. (1999a), extracted from galaxy and cluster catalogs and estimated in the range $\sim 20 - 200 h^{-1} \text{ Mpc}$. Secondly, on very large scales we assume the initial spectrum to be scale-invariant ($n = 1$) and COBE/DMR normalized, since this choice produces the best fit to previous CMB data for multipoles $l < 200$ (fortunately, it agrees with the prediction of the simplest version of the inflationary scenario, too). In the next section we shall describe two possible ways to match these pieces of the spectrum.

In this article, we show that such an empirical spectrum gives a possibility to explain the peculiar features of the BOOMERANG-98 and MAXIMA-I data without changing standard cosmology or the basic laws of physics. Also, we do not introduce non-scale invariant features in the power spectrum *ad hoc*, but only those required by

the observations. In addition to this initial spectrum, we assume certain priors: a spatially flat universe, the age of the universe between 12 and 14 Gyr and a negligible contribution from primordial gravitational waves to the COBE/DMR data. We considered models with different Hubble constant, cosmological constant, and baryon fraction. We computed the expected temperature anisotropy for each model and found the region of the parameter space that best fitted the BOOMERANG-MAXIMA data. In Section 2 we describe our methods and results. In Section 3 we find the cluster mass distribution. We calculate the initial power spectrum for our models in Section 4 and present the main results in Section 5.

2. TEMPERATURE ANISOTROPIES ON INTERMEDIATE ANGULAR SCALES

Temperature anisotropies are usually expressed in terms of spherical harmonics with coefficients a_{lm} . At a given angular scale l , the contribution of the matter power spectrum to the radiation temperature anisotropy is dominated by perturbations with the wavenumber $k \simeq (\pi/2)l/R_H$, where R_H is the radius of the present (post-inflation) particle horizon (in particular, $R_H = 9900 h^{-1} \text{ Mpc}$ for a flat Universe with the matter density parameter $\Omega_m = 0.3$). Note that only perturbations with wavenumbers $k > l/R_H$ contribute to the CMB radiation temperature at any l (for $l \gg 1$ and neglecting the integrated Sachs-Wolfe effect which is usually small for scales of interest here). Observations in the range $l \geq 200$ probe the amplitude of the matter power spectrum at recombination on the scales also probed by galaxy and cluster catalogs, i.e. on scales smaller than $200 h^{-1} \text{ Mpc}$. On very large scales ($k \leq 0.005 h \text{ Mpc}^{-1}$), temperature anisotropies are generated by fluctuations of the gravitational potential. The amplitude and the slope of the matter power spectrum in this region are strongly constrained by the COBE/DMR data. To compute CMB temperature anisotropies for $l = 2 - 1000$, and the matter power spectrum on scales $10^{-4} \leq k \leq 1 h \text{ Mpc}^{-1}$, we need to provide the initial (post-inflation) power spectrum in the whole wavenumber range.

We identify the matter power spectrum with the observational spectrum presented in Einasto et al. (1999a) (called HD for High Density as the mean power spectrum was derived including high-density regions such as clusters of galaxies) for $k \geq 0.035 h \text{ Mpc}^{-1}$. This spectrum is well approximated by a power law with the slope $n = -1.9$ for wavenumbers larger than $k_{pl} = 0.06 h \text{ Mpc}^{-1}$ up to $k \sim 0.4 h \text{ Mpc}^{-1}$ (the latter value is already sufficient for the calculation of CMB multipoles with $l < 1000$, so we use this fit for larger values of k , too):

$$P_{HD}(k) = P_{pl} (k/k_{pl})^{-1.9} h^{-3} \text{Mpc}^3, \quad (1)$$

where $P_{pl} = 1.02 \times 10^4 (\sigma_8/0.65)^2 h^{-3} \text{Mpc}^3$ is the value of the power spectrum at $k = k_{pl}$ (see Table 2, Einasto et al. 1999a). In the range $0.035 \leq k \leq 0.3 h \text{ Mpc}^{-1}$ this spectrum differs from the observed power spectrum of galaxies, by a scale factor or bias. On shorter scales, $k \geq 0.3 h \text{ Mpc}^{-1}$, the observed spectrum is corrected for non-linear evolution effects (for details see Einasto et al. 1999c); these corrections do not introduce any significant differences to the CMB spectra at the scales of

interest. Note that in this range, the spectrum of Einasto et al. (1999a, 1999c) is in good agreement with results obtained by other authors, for recent new data see Miller et al. (2001), among others. Since we do not know the exact value of the bias between the galaxy and matter power spectra, the value of k_{pl} is a free parameter of our model which is expressed in terms of σ_8 once the shape of $P(k)$ is fixed. On the other hand, on very large scales, $k < k_m = 0.03 \ h \text{ Mpc}^{-1}$, we accept the scale-invariant ($n = 1$) COBE normalized spectrum since it gives the best fit to CMB data for $l < 200$. The location of k_m is chosen to be in agreement with the observational cluster spectrum of Miller & Batuski (2000) and the de-correlated IRAS Point Source redshift catalog (PSCz) galaxy spectrum of Hamilton, Tegmark & Padmanabhan (2000).

In the intermediate range, $k_m \leq k \leq k_{pl}$, error bars are large and there is no complete agreement between different authors about the exact form of $P(k)$. For this reason, we use two different models of $P(k)$ in this region: one more conservative and another based on the Einasto et al. (1999a) data. In the first case we use at small scales the power law behavior given in (1). This spectrum is extrapolated until it crosses the linear COBE-normalized spectrum that is based on the primordial scale invariant spectral index $n = 1$ and evolved through recombination using cosmological parameters discussed above. On large scales the spectrum based on is $n = 1$ used. It was calculated using the CMBFAST program. This power spectrum is called HDL (L standing for linear extrapolation). In the second case we apply the observational HD spectrum from Einasto et al. (1999a) up to $k = 0.035 \ h \text{ Mpc}^{-1}$, i.e., up to the smallest wavenumber for which it contains reliable data. Then $P(k)$ is linearly matched to the scale invariant $n = 1$ COBE normalized spectrum at $k = k_m = 0.03 \ h \text{ Mpc}^{-1}$. For smaller k , we use the scale invariant spectrum as in the first case. The resulting spectrum has a distinct bump at $k = k_b$, and a depression in the whole region $k > k_m$, as compared to the COBE normalized $n = 1$ spectrum, see Fig 1a,b. Thus we call it HDB (B for bump). Notice that the difference between the two spectra is still within 1σ error bars.

The HDL spectrum is similar to those considered in Kanazawa et al. (2000) and Barriga et al. (2000). The HDB spectrum is more complicated, it is not monotonous. Its form is in agreement with the power spectrum proposed by Einasto et al. (1997); the existence of the bump at $k = 0.05 \ h \text{ Mpc}^{-1}$ (now understood to be a relative bump above a depression in the spectrum) could help to explain some quasi-periodic features in the large-scale distribution of Abell clusters noted in the latter and other papers. It is interesting that the double feature – the bump at $k = 0.05 \ h \text{ Mpc}^{-1}$ and the depression at $k \simeq 0.035 \ h \text{ Mpc}^{-1}$ – are seen in the Miller & Batuski (2000) and Hamilton, Tegmark & Padmanabhan (2000) data, too, though within 1σ error bars. Similar features have been reported in two recent preprints: Hoyle et al. (2001) found a small bump at $k \approx 0.06 \ h \text{ Mpc}^{-1}$ (assuming $\Omega_m = 0.3$) in the power spectrum of the 2dF QSO Redshift Survey, and Silberman et al. (2001) claimed a wiggle in the power spectrum with an excess at $k \sim 0.05 \ h \text{ Mpc}^{-1}$ and a deficiency at $k \sim 0.1 \ h \text{ Mpc}^{-1}$, based on peculiar velocities of galaxies from the Mark III and SFI catalogs. Bumps at $k \approx 0.05 \ h \text{ Mpc}^{-1}$ and $k \sim 0.2 \ h \text{ Mpc}^{-1}$ and depres-

sions (valleys) at $k \simeq 0.035 \ h \text{ Mpc}^{-1}$ and $k \sim 0.1 \ h \text{ Mpc}^{-1}$ have been confirmed by Miller, Nichol & Batuski (2001) in their analysis of power spectra of Abell and APM clusters of galaxies, and PSCz galaxies. Note, however, that there are no such features in the recent REFLEX X-ray cluster survey (Schuecker et al. 2000). Certainly, both HDL and HDB are non-scale-invariant spectra. Though we have arrived at them using purely empirical arguments, we shall discuss how they could have arisen in inflationary models in Section 4.

To compute the radiation and matter power spectrum at the present epoch we used the CMBFAST program developed by Seljak & Zaldarriaga (1996). Given a set of parameters and scale-invariant initial conditions of the type $\tilde{\delta}(k) = Ak^{(n-1)/2}$ for the rms Fourier amplitudes of the density contrast at horizon crossing, we obtained a matter power spectrum with spectral index n at large scales. Parameter A was normalized to reproduce the COBE/DMR amplitude. In this work, we assumed that a difference between the power spectrum predicted by a given cosmological model today, $P(k)$, and the observed power spectrum, $P_{HD}(k)$, was due to initial conditions only. Then, as all scales of interest are still in the linear regime, the initial rms Fourier amplitude of matter density perturbations that give rise to the observed spectrum is

$$\tilde{\delta}_{HD}(k) = \tilde{\delta}(k)(P_{HD}(k)/P(k))^{1/2}. \quad (2)$$

In this expression, the power spectra are evaluated at the present time, and the amplitude of $\tilde{\delta}_{HD}(k)$ is evaluated at the horizon crossing.

Our main goal is to determine if the B01 and M01 new measurements agree with the observed matter power spectrum and with the standard BBN. Therefore, we restricted our analysis of the parameter space to a rather limited set, centered upon the region that best fitted the CMB data before BOOMERANG-98 and MAXIMA-I data (see Tegmark & Zaldarriaga 2000a). We considered spatially flat models with and without cosmological constant ($\Omega_m + \Omega_\Lambda = 1$, $\Omega_m = \Omega_{CDM} + \Omega_B$), with matter density in the range $0.3 \leq \Omega_m \leq 1$, with $n = 1$ and baryon fraction $0.005 \leq \Omega_B h^2 \leq 0.035$ centered on the range suggested by Tytler et al. (2000). Particular attention was paid to models with a cosmological constant. We took the age of the Universe t_0 to be between 12 and 14 Gyr, in agreement with the recalibration of the cosmic ages made by Feast & Catchpole (1997) using new Hipparcos distance determinations, and from estimations of the age of globular clusters (Jimenez 1999). The resulting Hubble constant varied from $h \simeq 0.5$ to 0.75 , consistent with observations.

Models with a small mixture of massive neutrinos have also been discussed in the literature, but this component has little effect on the radiation power spectrum in the range considered here. However, it is important to realize that as neutrino free-streaming erases the matter power spectrum at small scales, they have an effect on the initial matter power spectrum computed using (2). If the dark matter is “cold” and $\Omega_m \simeq 1$ then the initial spectrum deviates strongly from scale invariant initial conditions. This is expected since the standard CDM has too

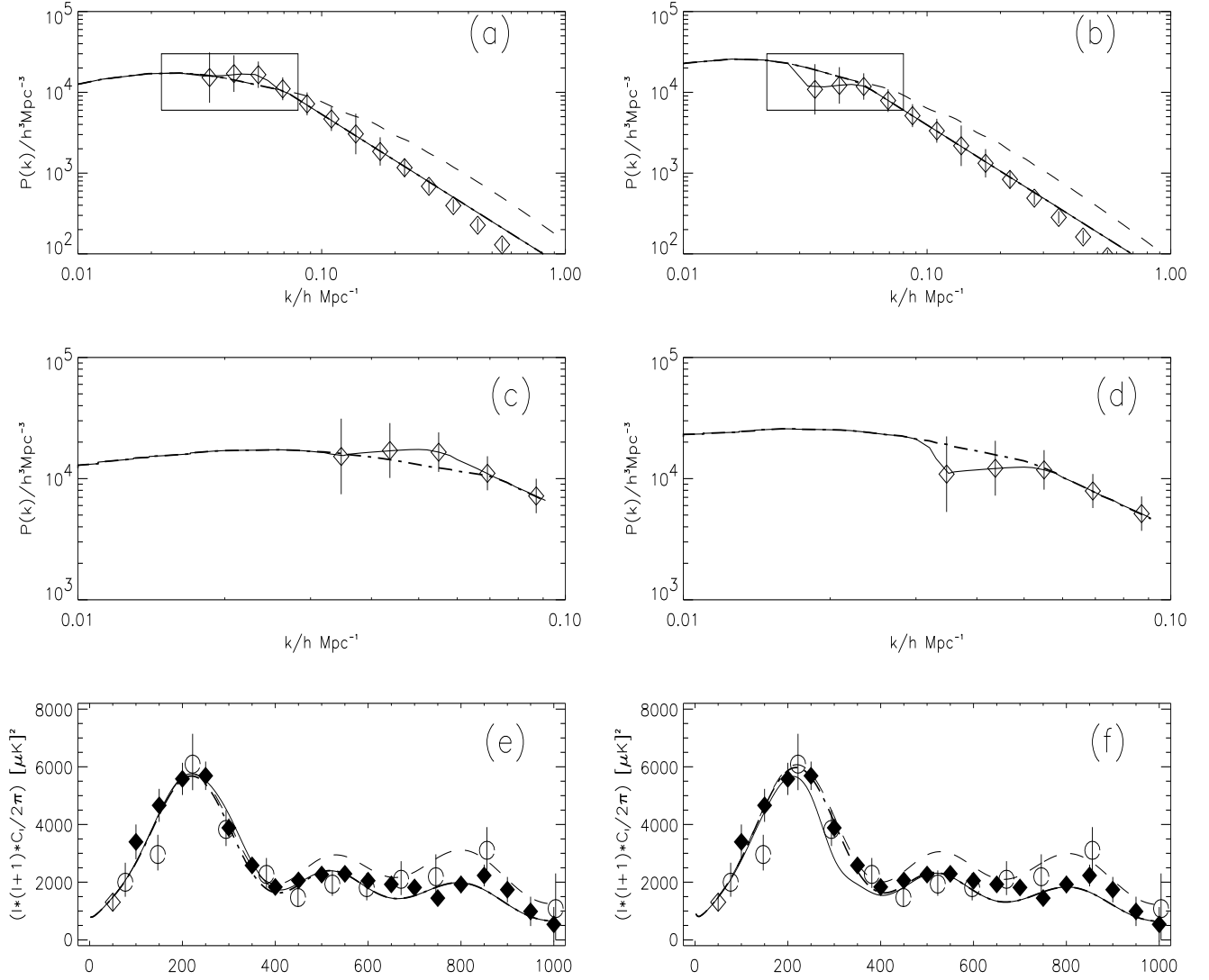


FIG. 1.— (a,b) Matter power spectrum of Λ CDM models with scale invariant (dashed line), HDB (solid line) and HDL (thick dot-dashed line) initial conditions. The matter density is $\Omega_m = 0.5$ in (a) and 0.3 in (b). The box encloses the region where the observed power spectrum is extended to match smoothly the scale invariant spectrum at large scales. Diamonds and bars represent the observed matter power spectrum $P_{HD}(k)$ and the associated 1σ error bar (data taken from Table 2 of Einasto et al 1999a). This area has been enlarged in (c,d) to show the difference between the spectra HDL and HDB. For clarity the scale invariant Λ CDM model is not plotted. (e,f) Radiation power spectrum of the same models. Filled diamonds and open circles correspond to B01 and M01 data, respectively.

TABLE 1

Position of the first maximum of the CMB spectrum

Model	$\Omega_m = 0.5$	$\Omega_m = 0.3$
Scale invariant	219	217
HDL	218	216
HDB	214	209

much power on small scales. If we assume that the ob-

served spectrum deviates only weakly from the Harrison-

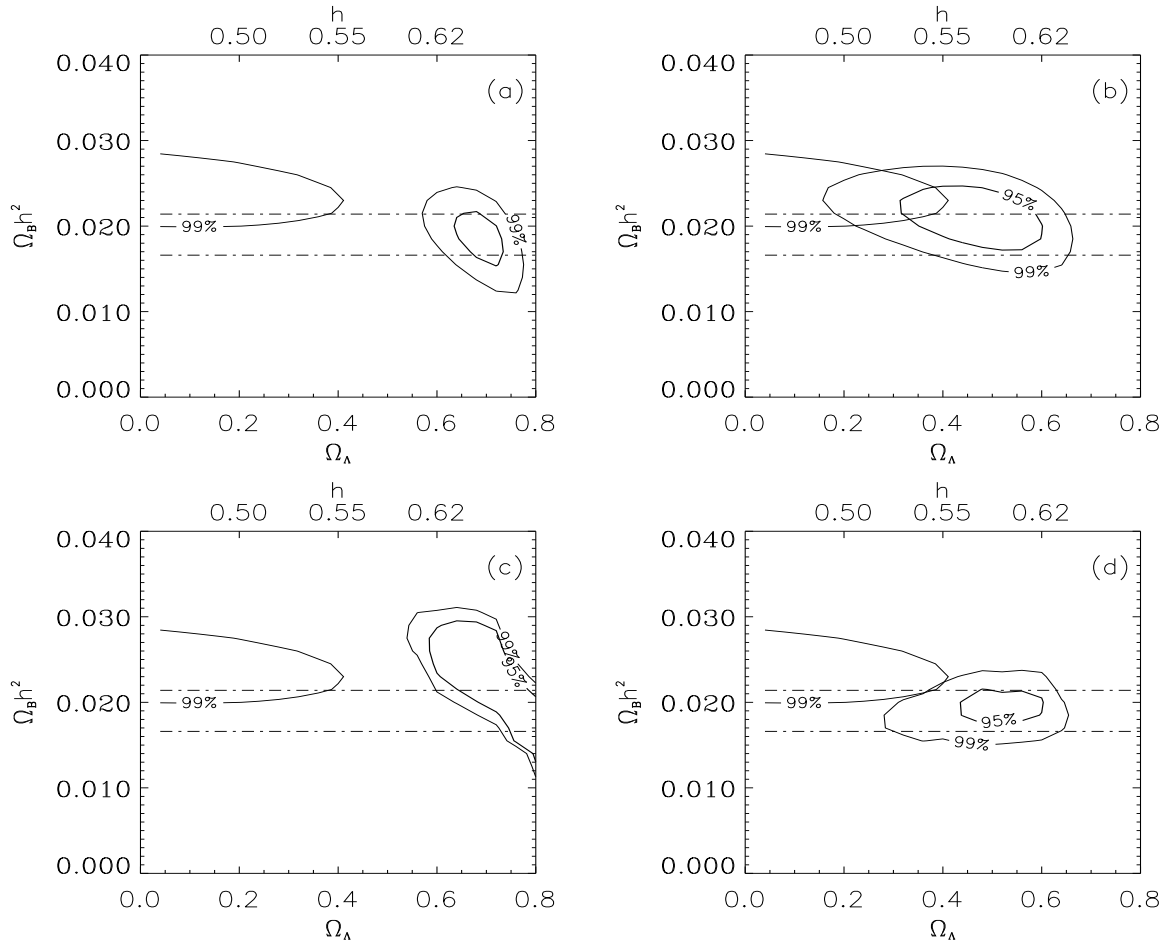


FIG. 2.— Goodness-of-fit contours of the likelihood function at 95% (thick solid line) and 99% (thin solid lines) confidence levels. The fit was performed using the newly released data B01, M01 up to $l \simeq 650$. No calibration uncertainties were included. Contours on the left side of panels correspond to scale invariant Λ CDM models and are shown for comparison; right contours correspond to HDL or HDB models. All models correspond to a Universe age of 14 Gyr and to matter power spectra with a $n = 1$ spectral index on large scales. Upper two panels: solid lines correspond to a HDL power spectrum with (a) $\sigma_8 = 0.65$ and (b) $\sigma_8 = 0.75$. Lower two panels: solid lines correspond to a HDB power spectrum with (c) $\sigma_8 = 0.65$ and (d) $\sigma_8 = 0.75$. Dot-dashed straight lines correspond to the 1σ BBN limits on the baryon fraction.

Zeldovich spectrum, then the theoretical power spectrum on scales smaller than the bump ($k \geq 0.05 h \text{ Mpc}^{-1}$) coincides with the observed spectrum only for a restricted set of cosmological parameters. In particular, demanding that the observed spectrum deviates only slightly from scale invariance, we fix the matter density parameter to be $\Omega_m \approx 0.3$ (if the non-baryonic dark matter is “cold”). A small mixture of “hot” dark matter would allow for a larger matter density (Einasto 2000 and Section 4 below).

In Figure 1, we present the COBE-normalized matter power spectra (upper panels a and b with an enlarged version in the middle panels c and d) and radiation power spectra (lower panels e and f) for three different types of spectra: scale invariant (dashed line), HDB (solid) and HDL (thick dot-dashed), for a universe with $t_0 = 14$ Gyr, the baryon fraction $\Omega_B h^2 = 0.02$ and the matter density $\Omega_m = 0.5$ (left panels) and $\Omega_m = 0.3$ (right panels). In this figure we use $\sigma_8 = 0.75$ in the left panel and $\sigma_8 = 0.65$ in the right panel. The HDL power spectrum follows Eq (1) till $k \simeq 0.08 h \text{ Mpc}^{-1}$ (for $\Omega_m = 0.5$), and till $k \simeq 0.06$ (for $\Omega_m = 0.3$) where it follows the Λ CDM spectrum. Then HDL coincides or is below the scale in-

variant power spectrum. The HDB spectrum follows the observed spectrum up to $k = 0.035 h \text{ Mpc}^{-1}$, and then is linearly extrapolated until it reaches the scale invariant spectrum at $k = 0.03 h \text{ Mpc}^{-1}$. It can be above or below the scale invariant spectrum. In the radiation spectra, the main differences between HDB and HDL are around the first Doppler peak. The data on the matter power spectrum was taken from Einasto et al. (1999a), while the CMB data is the latest M01 and B01 (this is also the data used to fit the models shown in Figure 2).

From the initial power spectrum, we compute the radiation power spectrum and compare the expected level of anisotropy with the CMB data. We used the radical compression of the cosmic microwave background data method described in Bond, Jaffe & Knox (2000). We computed the parameter space compatible with the newly released B01, M01 and, for comparison, with the earlier data recalibrated according to Jaffe et al. (2000). We restricted our study to $l \leq 650$ since it allows a better comparison with earlier parameter estimates. Further, above that scale the error bars are most affected by $\pm 13\%$ effective beam uncertainty and this uncertainty is not included in the published

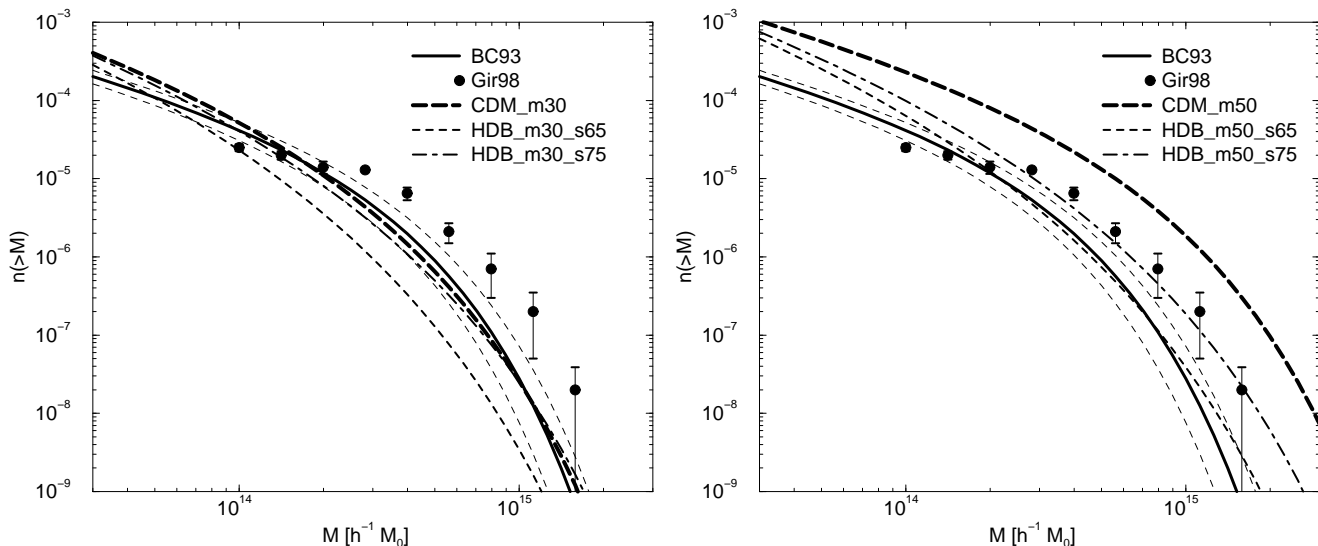


FIG. 3.— Cluster mass functions for models with the density parameter $\Omega_m = 0.3$ and $\Omega_m = 0.5$ are plotted in the left and right panels, respectively. The observed cluster mass functions are given according to Bahcall & Cen (1993) (thick solid line indicates the data and thin solid lines the width of the error corridor) and Girardi et al. (1998). Model functions are given for scale-invariant CDM models (with a cosmological constant), and for our models HDB with a bump for $\sigma_8 = 0.65$ and $\sigma_8 = 0.75$.

error bars. In Fig 2 we give the contours at the 95% (2σ) and 99% confidence levels for Λ CDM models with scale invariant, HDB and HDL power spectra. The figure corresponds to a fit to the B01, M01 data. On the upper axis we plot the corresponding Hubble constant. All models presented in Fig. 2 correspond to the slope $n = 1$ on very large scales. Figure 2a shows that scale invariant models are marginally consistent with the BBN bounds only at the 99% level. Our results also indicate that HDL and HDB models with $t_0 = 12$ Gyr (not shown in the figure) require $\Omega_\Lambda > 0.75$ (at the 2σ level), hardly compatible with direct measurements of $\Omega_m = 1 - \Omega_\Lambda$. On the contrary, models with $t_0 = 14$ Gyr lay inside the standard BBN limits and fit the recent CMB data very well for both the HDL and HDB spectra. We repeated the same analysis with the original recalibrated data. In this case, the contours were wider and scale invariant models become compatible with the BBN bound. Let us remark that, as seen in Figure 1, BOOMERANG-98 and MAXIMA-I have different amplitudes at the scale of the second acoustic peak, thus it is harder for the models to fit them both. However, in both cases the contours for HDL and HDB spectra were centered on the same region of the parameter space, implying that our results are robust.

In Table 1 we give the position of the maximum of the first acoustic peak for the models presented in Fig. 1. Let us remark that since, in general, the HDB and HDL spectra have less power than a scale invariant model with the same cosmological parameters, the position of the maximum of the first acoustic peak is shifted with respect to the scale invariant model. This effect is easily explained by the $k-l$ correspondence given at the beginning of this section: the depression in the HDB spectrum relative to the scale-invariant spectrum in the range $k = 0.03 - 0.05 h \text{ Mpc}^{-1}$ results in the decrease of the corresponding angular radi-

ation spectrum for $l = 200 - 500$ (if $\Omega_m = 0.3$). This effect explains the position of the first Doppler peak without invoking a small positive spatial curvature.

3. CLUSTER MASS FUNCTION

Another important constraint of cosmological models is the cluster mass function. This function is rather sensitive to cosmological parameters and features in the power spectrum on intermediate and small scales which have the highest weight in the cluster formation process. To check our results we calculated the cluster mass function using the Press-Schechter (1974) method. Mass functions were found for two sets of models; we used the Hubble constant $h = 0.65$ and the baryon fraction $\Omega_B = 0.05$, the matter density was taken $\Omega_m = 0.3$ and $\Omega_m = 0.5$, varying the density of the cold dark matter and the vacuum energy (cosmological constant) respectively. The Hubble constant used is a compromise between recent new estimates by different teams (Parodi et al. 2000, Sakai et al. 2000). As before, we used only spatially flat models ($\Omega_m + \Omega_\Lambda = 1$); the slope of the spectrum on small scales was taken to be $n = -1.9$, and the spectrum amplitude parameters $\sigma_8 = 0.65, 0.75$ were used.

The results of calculations are shown in Figure 3. The HDB model with $\Omega_m = 0.3$ and $\sigma_8 = 0.65$, that fits the CMB data rather well, has a too low abundance of clusters while the scale invariant Λ CDM model and HDB model with $\Omega_m = 0.3$ and $\sigma_8 = 0.75$ lie within the range allowed by observations. It is not surprising that the last two models coincide since the Λ CDM model with $\Omega_m = 0.3$ has $\sigma_8 = 0.78$, very close to our HDB model with $\Omega_m = 0.3$ and $\sigma_8 = 0.75$. This σ_8 value is in good agreement with other independent estimates (Einasto et al. 1999b, Van Waerbeke et al. 2001). The Λ CDM model with $\Omega_m = 0.5$ has too high abundance of clusters over the whole mass

range (about a factor of ten). In contrast, $\Omega_m = 0.5$ HDB models with both values of σ_8 have cluster mass functions which lie within the allowed region. In other words, cluster mass functions of HDB models are rather insensitive to the density parameter. This result is expected since our HDB models with both density values (but an identical Hubble parameter) are identical on medium and small scales, $k \geq 0.06$, which have the highest weight in determining the cluster mass function.

Using the preprint version of this paper, Gramann & Hütsi (2001) investigated properties of models similar to our models HDL, fixing the break of the power spectrum at $k_{pl} = 0.05 h \text{ Mpc}^{-1}$ (instead of at $0.06 h \text{ Mpc}^{-1}$). They confirmed our results that the amplitude of the second and third peak in the radiation power spectrum decreases and fits the CMB data better. Gramann & Hütsi also calculated the cluster mass function with the Press-Schechter method and found that the amplitude of the power spectrum of their models was too low which lead to a low cluster mass function incompatible with observations. They suggested to use an initial power spectrum which has a depression around $k = 0.1 h \text{ Mpc}^{-1}$ and an increased amplitude starting from $k = 0.2 h \text{ Mpc}^{-1}$. Models with such spectra were investigated by Suhonenko & Gramann (1999). Such spectra also yield satisfactory agreement both with the observed cluster mass function and with the recent CMB spectrum data. A similar power spectrum was found in the recent paper by Silberman et al. (2001) based on the analysis of galaxy peculiar velocities, and by Miller, Nichol & Batuski (2001) based on the analysis of power spectra of Abell and APM clusters of galaxies, and IRAS Point Source redshift catalog galaxies.

To bring our HDB model with $\Omega_m = 0.3$ and $\sigma_8 = 0.75$ into a better agreement with the CMB data, perhaps a model with a second feature on small scales is needed, as suggested by Gramann & Hütsi (2001) and Miller, Nichol & Batuski (2001). The latter authors considered the presence of two bumps and two depressions (valleys) in the observed power spectrum as evidence for baryonic fluctuations, as discussed by Eisenstein et al. (1998). However, this hypothesis encounters one problem: the position of the first baryonic bump on the matter power spectrum is expected at the wavenumber $k \approx 0.07 h \text{ Mpc}^{-1}$, whereas the observed bump is located at the wavenumber $k \approx 0.05 h \text{ Mpc}^{-1}$. The bump at $k = 0.05 h \text{ Mpc}^{-1}$ corresponds to the scale of the supercluster-void network, $\sim 120 h^{-1} \text{ Mpc}$, as seen in the distribution of high-density regions in a pencil-beam near galactic poles (Broadhurst et al. 1990), and in the distribution of clusters of galaxies (Einasto et al. 1997a, 1997b). More accurate data are needed to decide whether the observed features of the power spectrum are due to a high baryon fraction or are primordial effects. At present, we are inclined to accept the second alternative since, without requiring new physics, it fits the CMB data within the BBN bounds quite naturally.

4. POST-INFLATION INITIAL CONDITIONS

Though we did not require *a priori* that our initial spectra should be “explicable” by any theoretical model, it appears that, for $\Omega_m \approx 0.3$, the form of the HDB spectrum suggests an inflationary model with a fast phase transition occurring approximately 50 e-folds before the end of

inflation, similar to those with a sudden jump in an inflaton potential which were considered in Starobinsky (1992) and Adams, Ross & Sarkar (1997); see also the recent paper by Adams, Cresswell & Easther (2001) (which appeared after the preprint version of the present paper was sent to the archive) where a very similar spectrum is obtained. As for the simpler HDL spectrum, and for the HDB spectrum with $\Omega_m \approx 0.5$, it is rather typical for double inflationary models, see, e.g., the models in Polarski & Starobinsky (1992), Gottlöber, Mückel & Starobinsky (1994), as well as the models proposed in Kanazawa et al. (2000) and Barriga et al. (2000). Also, a similar step-like spectrum appears in the case when the inflaton potential has a jump of its first derivative (Starobinsky 1992). Thus, relatively small changes in cosmological parameters and in the present form of $P(k)$ may lead to significantly different models of the phase transition during inflation.

To elaborate this point further, let us compute the ratio of power spectra:

$$S(k) = P_{HDB}(k)/P_{CDM}(k). \quad (3)$$

Here, we use the power spectrum with a bump, $P_{HDB}(k)$, and the scale-invariant Λ CDM power spectrum $P_{CDM}(k)$, calculated for the same set of cosmological parameters as the spectrum with a bump. The function $S(k)$ characterizes the deviation of our accepted spectrum from the scale-invariant case, namely, the initial spectrum $P_0(k) \propto kS(k)$. In Fig. 4 we plot the ratio $S(k)$ for a Hubble constant $h = 0.65$, baryon density $\Omega_B = 0.05$, and $\sigma_8 = 0.65$ and $\sigma_8 = 0.75$ for three different values of the matter density. We do not plot the ratio using the HDL spectrum since $S(k)$ is the same as for HDB for $k \geq 0.06 h \text{ Mpc}^{-1}$ and coincides with the scale invariant case ($S(k) = 1$) for $k \lesssim 0.05 h \text{ Mpc}^{-1}$ as explained in Section 2.

By construction, on large scales the HDB spectrum is identical to the scale-invariant Λ CDM spectrum, i.e., $S(k) = 1$. Deviations start at $k \simeq 0.03 h \text{ Mpc}^{-1}$: all initial spectra have a depression around $k = 0.035 h \text{ Mpc}^{-1}$, a bump at $k = 0.05 h \text{ Mpc}^{-1}$, and an approximate power law dependence on smaller scales. The initial spectrum given in (3) depends only slightly on the σ_8 parameter. For the matter density $\Omega_m = 0.3$, deviations of our accepted spectra from the scale-invariant spectrum are moderate and localized near $k = 0.05 h \text{ Mpc}^{-1}$. We call these spectra “locally broken-scale-invariant”. In contrast, for the matter density $\Omega_m = 0.5$ and $\Omega_m = 1.0$, deviations on small scales become large. Even if we do not include a small fraction of hot dark matter, the function $S(k)$ can be brought closer to unity on the scale interval $0.06 \leq k \leq 0.4 h \text{ Mpc}^{-1}$ using a tilted spectrum. Tilted spectra have been often used to explain the observed power spectrum of galaxies. This helps to bring $S(k) \approx 1$ over the whole range only for $\Omega_m = 0.3$. For higher values of the matter density, the tilt needed becomes too large and is excluded using the COBE data, that suggest $n = 1 \pm 0.1$.

To summarize, the CMB data in combination with the matter spectrum and cluster abundance favor the density parameter $\Omega_m \simeq 0.3$. For this density value, the initial matter power spectrum is approximately scale invariant. Figure 2 indicates that for $\Omega_m \simeq 0.3$ the CMB data prefers $\sigma_8 = 0.65$ for both the HDL and HDB spectra, while the value of $\Omega_m \simeq 0.5$ is preferred by the data when $\sigma_8 = 0.75$.

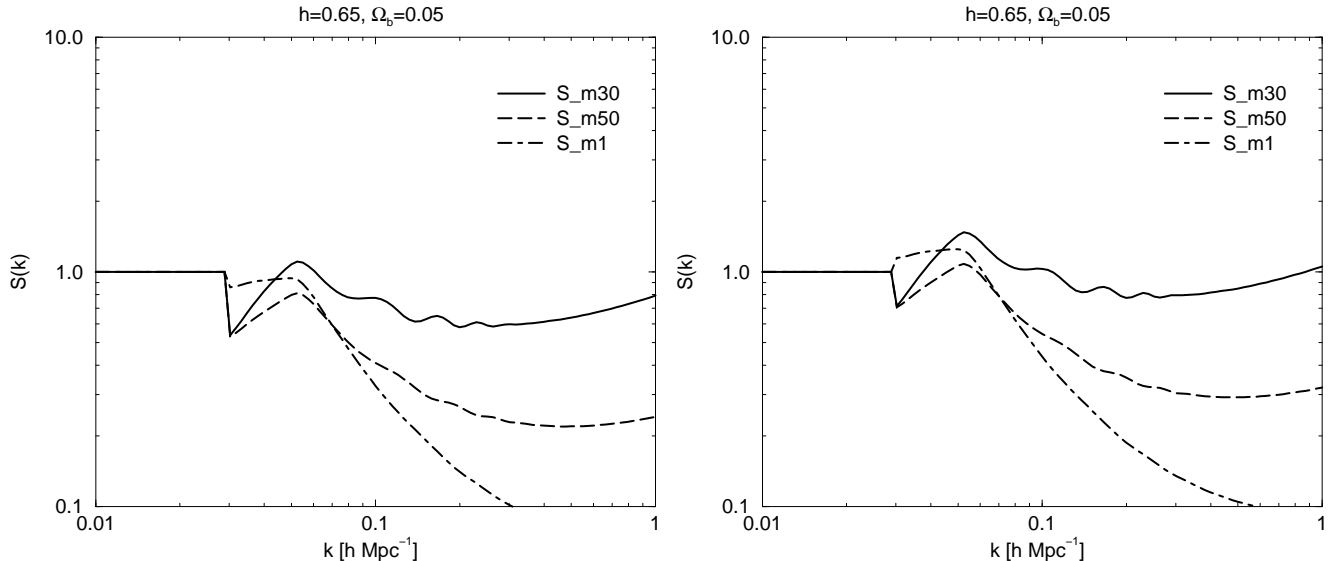


FIG. 4.— The initial power spectrum, expressed as the ratio of our adopted HDB spectrum to the scale-invariant Λ CDM spectrum, $S(k) = P_{HDB}(k)/P_{CDM}(k)$. The initial power spectrum is calculated for 3 values of the matter density, $\Omega_m = 0.3, 0.5, 1.0$. In the left panel $\sigma_8 = 0.65$, in the right panel $\sigma_8 = 0.75$.

However, this density value exceeds considerably the value preferred by other data sets (Perlmutter et al. 1998, Riess et al. 1998, see also Ostriker & Steinhardt 1995), and also requires large deviations from the scale-invariant initial conditions.

5. CONCLUSIONS

We have shown that the amplitude of the second acoustic peak measured by BOOMERANG-98 and MAXIMA-I is compatible both with the standard BBN and with the matter power spectrum obtained from galaxy and cluster catalogs, if we accept a non-scale-invariant power spectrum. If we assume that the age of the Universe is 14 Gyr, and the initial power spectrum has an index close to the Harrison-Zeldovich value, $n = 1 \pm 0.1$, then our best fit within the standard BBN bound gives for the matter density parameter, $0.3 \leq \Omega_m \leq 0.5$. If we demand that the matter power spectrum yields a correct cluster abundance, then the matter density is further constraint: $\Omega_m \approx 0.3$.

The amplitude of the second peak in the radiation power spectrum and the shape of the matter power spectrum can be both simultaneously explained using models with the standard baryon abundance. Since our accepted spectra have less power than the scale-invariant model with the same cosmological parameters (and before the new data was available) we had predicted a low third acoustic peak. This testable prediction of our models can be clearly seen in Figs 1(e), 1(f): the third acoustic peak is not higher (and typically lower) than the second peak. While the original paper was being refereed, Netterfield et al. (2001) extended the analysis of the BOOMERANG-98 data to higher multipoles and indeed found an amplitude of the third Doppler peak being of a similar amplitude as the second one. However, Lee et al. (2001) claim to have seen a larger third peak in the MAXIMA-I data. In this respect, let us remark that HDL and HDB spectra coincide for $k > 0.05 h \text{ Mpc}^{-1}$, their CMB angular spectra are prac-

tically the same for $l > 500$ (if $\Omega_m = 0.3$) while in scale invariant models with a high baryon abundance and models with leptonic asymmetry the third peak is higher than the second. As the data around the third peak improves, its amplitude will be an important test on our models.

Our second result is the shift of the first acoustic peak to a smaller value of l as compared to the scale-invariant spectrum (see Table 1). This effect is especially noticeable in the case of the HDB spectrum. This brings the BOOMERANG-MAXIMA data to excellent agreement with a spatially flat Universe, removing the need for a slightly positive spatial curvature. Also, the cluster mass function for the HDB type models is well within the observational error bars.

Finally, it is important to notice that the data do not contradict the existence of a bump and a depression of the HDB spectrum. The existing CMB data are not sufficient to determine the detailed form of the matter power spectrum in the range $0.03 < k < 0.06 h \text{ Mpc}^{-1}$ where we expect a deviation from the scale-invariant spectrum to be most significant. Analysis of the data around the third peak will be useful to determine the amplitude of the matter power spectrum at small scales, but is not relevant for the question about the feature. But before this analysis can be carried out, the discrepancy between Maxima and other experiments should be resolved in some way, i.e., is the third peak high or low.

Acknowledgements: We thank Mirt Gramann and Enn Saar for discussion. F. A.-B. acknowledges the financial support of the Junta de Castilla y León (project SA 19/00B) and the Ministerio de Educación y Cultura (project BFM2000-1322). J.E. was supported by Estonian Science Foundation grant 2625. A.S. was partly supported by the Russian Foundation for Basic Research, grant 99-02-16224, and by the Russian Research Project “Cosmophysics”.

REFERENCES

- Adams, J., Cresswell, B. & Easther, R. 2001, preprint (astro-ph/0102236)
- Adams, J.A., Ross, G.G. & Sarkar, S. 1997, Nucl. Phys. B., 391, 405
- Avelino, P.P., Martins, C.J.A.P., Rocha, G. & Viana, P. 2000, Phys. Rev. D 62, 123508
- Bahcall N.A., Cen R., 1993, ApJ, 407, L49
- Balbi, A. et al. 2000, ApJ 545, L1
- Barriga, J., Gaztañaga, E., Santos, M.G. & Sarkar, S. 2000, preprint (astro-ph/0011398)
- Battye, R.A., Crittenden, R. & Weller, J. Phys. Rev. D 63 (2001) 043505
- Bond, J.R. et al. 2000, preprint (astro-ph/0011379)
- Bond, J.R., Jaffe, A.H. & Knox, L. 2000, ApJ, 533, 19. (<http://flight.uchicago.edu/knox/radpack.html>)
- Bouchet, F.R., Peter, P., Riazuelo, A. & Sakellariadou, M. 2000, preprint (astro-ph/0005022)
- Broadhurst, T. J., Ellis, R. S., Koo, D. C., and Szalay, A. S., 1990, Nature, 343, 726
- Chung, D.J.H., Kolb, E.W., Riotto, A., & Tkachev, I.I., 2000, Phys. Rev. D 62, 043508, (hep-ph/9910437)
- de Bernardis, P. et al. 2000, Nature, 404, 955
- Einasto, J. 2000, in *Dark2000: Dark Matter in Astro and Particle Physics*, eds. H.V. Klapdor-Kleingrothaus & B. Majorovits, Springer, (in Press), (astro-ph/0011333)
- Einasto, J., Einasto, M., Gottlöber, S., Müller, V., Saar, V., Starobinsky, A.A., Tago, E., Tucker, D. & Andernach, H. 1997a, Nature, 385, 139
- Einasto, J., Einasto, M., Tago, E., Starobinsky, A. A., Atrio-Barandela, F., Müller, V., Knebe, A., Frisch, P., Cen, R., Andernach, H. & Tucker D. 1999a, ApJ, 519, 441
- Einasto, J., Einasto, M., Tago, E., Müller, V., Knebe, A., Cen, R., Starobinsky, A. A., Atrio-Barandela, F. 1999b, ApJ, 519, 435
- Einasto, J., Einasto, M., Tago, E., Starobinsky, A.A., Atrio-Barandela, F., Müller, V., Knebe, A. & Cen, R. 1999c, ApJ, 519, 469
- Einasto, M., Tago, E., Jaaniste, J., Einasto, J., & Andernach, H., 1997b, *Astron. and Astrophys. Suppl.* **123** 119
- Eisenstein, D.J., Hu, W., Silk, J., & Szalay, A.S. 1998, ApJ, 494, L1
- Feast, M.W. & Catchpole, R.M. 1997, MNRAS, 286, L1
- Girardi M., Borgani S., Giuricin G., Mardirossian F., Mezetti M. 1998, ApJ, 506, 45
- Gottlöber, S., Mucket, J. & Starobinsky, A.A. 1994, ApJ 434, 417
- Gramann, M. & Hütsi, G. 2001, MNRAS, (in press), (astro-ph/0102466)
- Griffiths, L.M., Silk, J. & Zaroubi, S. 2000, preprint (astro-ph/0010571)
- Halverson, N.W. et al. 2001, ApJ (submitted), (astro-ph/0104489). D01
- Hamilton, A.J.S., Tegmark, M. & Padmanabhan, N. 2000, MNRAS, 317, L23.
- Hanany, S. et al. 2000, ApJ 545, L5
- Hannestad, S., Hansen, S.H. & Villante, F.L. 2000, preprint (astro-ph/0012009)
- Hoyle, F. et al. 2001, MNRAS (submitted) preprint (astro-ph/0102163)
- Jaffe, A.H. et al. 2000, preprint (astro-ph/0007333)
- Jimenez, R. 1999, in *Dark Matter in Astrophysics and Particle Physics*, eds. H.V. Klapdor-Kleingrothaus & L. Baudis, Inst. Phys. Publ., Bristol & Philadelphia, p. 170, (astro-ph/9810311)
- Kanazawa, T., Kawasaki, M., Sugiyama, N. & Yanagida, T. 2000, Phys. Rev. D, 61, 023517
- Lange, A. E. et al. 2001, Phys. Rev. D 63 042001, preprint (astro-ph/0005004)
- Lesgourgues, J. & Peloso, M. 2000, Phys. Rev. D, 62, 81301
- Lee, A.T., et al. 2001, ApJ (submitted), (astro-ph/0104459). M01
- McGaugh, S. 2000, ApJ 531, L33
- Miller, C.J. & Batuski, D.V. 2000, ApJ (in press), preprint (astro-ph/0002295)
- Miller, C.J., Nichol, R.C., & Batuski, D.V. 2001, ApJ (in press) preprint (astro-ph/0103018)
- Netterfield, C.B., et al. 2001, ApJ (submitted), (astro-ph/0104460). B01
- Ostriker, J.P., & Steinhardt, P.J. 1995, Nature, 377, 600
- Parodi, B.R., Saha, A., Sandage, A., & Tammann, G.A., 2000, ApJ, 540, 634, (astro-ph/0004063)
- Peebles P.J.E., Seager, S. & Hu, W. 2000, ApJ, 539, L1
- Perlmutter, S., et al. 1998, ApJ 517, 565
- Polarski, D. & Starobinsky, A.A. 1992, Nucl. Phys. B, 385, 623
- Press W.H., Schechter P. 1974, ApJ, 187, 425
- Riess, A.G., et al. 1998, *Astron. J.*, 116, 1009
- Sakai, S., Mould, J. R., Hughes, S.M.G. et al. 2000, ApJ, 529, 698, (astro-ph/9909269)
- Schuecker, P. et al. 2000, A&A, 368, 86, (astro-ph/0012105).
- Seljak, U. & Zaldarriaga, M. 1996, ApJ, 469, 437
- Silberman, L., Dekel, A., Eldar, A. & Zehavi, A. 2001, preprint (astro-ph/0101361)
- Starobinsky, A.A. 1992, JETP Lett., 55, 489
- Suhhonenko, I., Gramann, M., 1999, MNRAS, 303, 77
- Tegmark, M. & Zaldarriaga, M. 2000a, ApJ, 544, 30; preprint (astro-ph/0002091)
- Tegmark, M. & Zaldarriaga, M. 2000b, Phys. Rev. Lett., 85, 2240
- Tegmark, M., Zaldarriaga, M. & Hamilton, A.J.S. 2000, preprint (astro-ph/0008167)
- Tytler, D., O'Meara, J.M., Suzuki, N. & Lubin, D. 2000, Phys. Scr., 85, 12
- Van Waerbeke, L., Mellier, Y., Radovich, M., Bertin, E., Dantel-Fort, M., McCracken, H.J., Le Fevre, O., Foucaud, S., Cuillandre, J.-C., Erben, T., Jain, B., Schneider, P., Bernardeau, F., & Fort, B. 2001, A&A (in press), (astro-ph/0101511)
- Wang, Y., & Mathews, G. 2000, preprint (astro-ph/0011351)
- White, M., Scott, D. & Pierpaoli, E. 2000, ApJ 545, 1